# 176. Stereoselectivity in Reactions of Metal Complexes

Part XV[1])

## Structure and Stability of Chiral Cobalt(III) Complexes with Pentadentate Ligands

by **Klaus Bernauer***, **Helen Stoeckli-Evans**, **Deirdre Hugi-Cleary**, **Hermann J. Hilgers**, **Habib Abd-el-Khalek**, **Joëlle Porret**, and **Jean-Jacques Sauvain**

Institut de Chimie de l'Université de Neuchâtel, Av. de Bellevaux 51, CH–2000 Neuchâtel

(17.VII.92)

The syntheses and characterization of four new linear pentadentate ligands and their $Co^{III}$ complexes are described: *N,N'*-[(pyridine-2,6-diyl)bis(methylene)]bis[sarcosine] (sarmp), *N,N'*-[(pyridine-2,6-diyl)bis(methylene)]bis[(*R*)- or (*S*)-proline] ((*R,R*)- or (*S,S*)-promp), *N,N'*-[(pyridine-2,6-diyl)bis(methylene)]bis[*N*-(methyl)-(*R*)- or (*S*)-alanine] ((*R,R*)- or (*S,S*)-malmp); 2,2'-[pyridine-2,6-diyl]bis[(*S*)- or *rac*-*N*-(acetic acid)pyrrolidine] ((*S,S*)- or *rac*-bapap). The complexes were characterized and, with but one exception, complex formation is stereospecific: *Δ-exo*-(*R,R*) (or *Δ-exo*-(*S,S*)) for promp and *Δ*-(*R,R*) (or *Δ*-(*S,S*)) for bapap. The exception is [Co((*R,R*)- or (*S,S*)-malmp)$H_2O$]$ClO_4$ for which two forms are obtained, to which *Δ-endo*-(*R,R*) (or *Δ-endo*-(*S,S*)) and, tentatively, *Δ-unsymmetric*-(*R,R*)- (or *Δ-unsymmetric*-(*S,S*)-) configurations are assigned. X-Ray crystal structures are presented for the complexes [Co(sarmp)$H_2O$]$ClO_4$, [Co((*S,S*)-promp)$H_2O$]$ClO_4$, [Co(*rac*-bapap)$H_2O$]$ClO_4$ and *endo*-[Co(*rac*-malmp)$H_2O$]$ClO_4$. Ligand acid dissociation and $Co^{II}$ and $Fe^{II}$ complex-formation constants are reported.

**Introduction.** – Recent reviews of stereoselective electron-transfer reactions [2] [3] attest to the intense activity in this field since the first clear demonstration of stereoselectivity in 1980 [4]. The chirality of most of the complexes studied is determined by the arrangement of achiral, bidentate (en, oxo, phen) or multidentate ligands around the metal centre, and stereoselectivity can only be shown for inert coordination centres. Few examples are known of electron-transfer studies using optically active stereospecific ligands with labile metal ions, where one of the major problems is that of maintaining chirality in a substitution labile complex.

We have shown [5] [6] that ligands with the basic pentadentate framework illustrated in *Fig. 1* form metal complexes of a given absolute configuration with labile as well as inert metal ions. These types of ligands, insofar as ligand-exchange reactions can be excluded, can be used for stereoselectivity studies independently of the degree of lability of the metal complex. A variety of substituents can be introduced into the $C_2$ framework of the ligand.

This report concerns four new such pentadentate ligands: *N,N'*-[(pyridine-2,6-diyl)-bis(methylene)]bis[sarcosine] (sarmp); *N,N'*-[(pyridine-2,6-diyl)bis(methylene)]bis[proline] (promp), *N,N'*-[(pyridine-2,6-diyl)bis(methylene)]bis[*N*-methylalanine] (malmp),

[1]) Part XIV: [1].

| $R^1$ | $R^2$ | $R^3$ | Ligand abbreviation |
|---|---|---|---|
| Me | Me | H | bamap |
| H | H | Me | alamp |
| H | $-CH_2CH_2CH_2-$ | | promp |
| H | Me | Me | malmp |
| H | Me | H | sarmp |
| $-CH_2CH_2CH_2-$ | | H | bapap |
| H | Me | $Me_2CH$ | valmp |

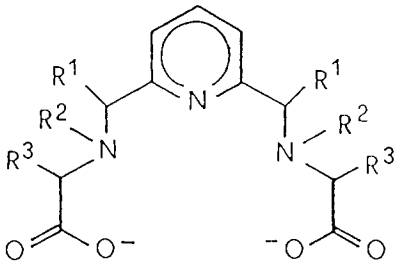

Fig. 1. *Basic framework of the stereospecific pentadentate ligands studied in this work*

and 2,2′-[pyridine-2,6-diyl]bis[*N*-(acetic acid)pyrrolidine] (bapap), and their corresponding $Co^{III}$ complexes. These four ligands complete a series of substitution inert chelates formed in a stereospecific way by systematic variation of the substituents on the basic framework illustrated in *Fig. 1*. sarmp is the only ligand of the series without any optically active C-atom: it has a Me group on each N-atom, which then becomes chiral upon coordination to a metal ion and, for this reason, can only be used for stereoselective studies with inert coordination centres. This ligand is complementary to alamp (*N*,*N*′-[(pyridine-2,6-diyl)bis(methylene)]bis[alanine]), which has a Me group on each C(α)-atom of the aminocarboxylate moiety. Malmp and promp are substituted on both the N- and C-atoms. In the case of malmp, the substituents are independent Me groups, whereas for promp, they are part of a five-membered ring and thus are held in a fixed position in the corresponding $Co^{III}$ complexes. The same similarity exists between bamap (*N*,*N*′-[(pyridine-2,6-diyl)bis(1-ethyl)]bis[sarcosine]) and bapap (see *Fig. 1*).

**Results and Discussion.** – 1. *Structures.* X-Ray crystal structures for [Co((*S*,*S*)-promp)$H_2O$]$ClO_4$, [Co(sarmp)$H_2O$]$ClO_4$, and [Co(*rac*-bapap)$H_2O$]$ClO_4$ are shown in *Fig. 2*. Each molecule is illustrated in such a way as to highlight some salient feature: fluxionality of C(16) in [Co((*S*,*S*)-promp)$H_2O$]$^+$, distortion of the N(3)–Co–N(2) plane in [Co(sarmp)$H_2O$]$^+$ and orientation of the $CH_2$ groups in [Co(*rac*-bapap)$H_2O$]$^+$. Selected bond distances and angles are listed in *Table 1*, along with values for [Co(*rac*-bamap)$H_2O$]$PF_6$, given for comparison [6]. Data for [Co(*rac*-malmp)$H_2O$]$ClO_4$, which will be discussed later, are included.

From *Table 1* and *Fig. 2*, it can be seen that the basic arrangement of the chelate rings in the four complexes is very similar. In all cases, the coordination sphere of the Co-atom is a distorted octahedral with a successive chelate ring arrangement of the fpf type [5].

The pyridine ring in the [Co((*S*,*S*)-promp)$H_2O$]$^+$ complex (*Fig. 2, a*) is twisted about the N(2)–N(1)–N(3) plane by 20.3°, and the $H_2O$ molecule deviates by 2.4° from the N(1)–Co axis. The N(1)–Co–N(2) angle is 82.24°, and the dihedral angle between the planes N(2)–Co–O(1) and N(3)–Co–O(3) is 16.0°, which indicates some distortion. This backward folding of the chelate rings is an important feature for the possible interactions between the substituents of the N- and/or the C(α)-atom of the reacting species in the transition state during electron-transfer reactions between complexes of this type.

An interesting feature of [Co((*S*,*S*)-promp)$H_2O$]$^+$ is the fluxionality observed for C(16) in one of the pyrrolidine rings. The atom is disordered over a distance of 1.2 Å between two chosen positions on either side of the N(3)–C(12)–C(17)–C(9) plane, each

Table 1. *Selected Bond Lengths* [Å] *and Angles* [°] *for* $Co^{III}$ *Complexes with Stereospecific Pentadentate Ligands*

| | $[Co(L)H_2O]ClO_4$ | $[Co(L)H_2O]ClO_4$ | $[Co(L)H_2O]ClO_4$ | $[Co(L)H_2O]PF_6$ | $[Co(L)H_2O]ClO_4$ |
|---|---|---|---|---|---|
| L | (*S*,*S*)-promp | sarmp | *rac*-bapap | *rac*-bamap | *rac*-malmp |
| Co–N(1) | 1.843(3)[a]) | 1.840(4) | 1.836(3) | 1.838(7) | 1.835(3) |
| Co–N(2) | 1.983(3) | 1.978(4) | 1.980(3) | 2.000(5) | 1.984(3) |
| Co–N(3) | 1.971(3) | 1.976(4) | 1.978(3) | 2.000(5) | 1.976(3) |
| Co–O(1) | 1.886(3) | 1.883(3) | 1.900(2) | 1.865(4) | 1.869(2) |
| Co–O(3) | 1.868(3) | 1.868(3) | 1.879(2) | 1.865(4) | 1.895(2) |
| Co–O(W) | 1.969(3) | 1.919(4) | 1.919(3) | 1.909(8) | 1.917(3) |
| N(1)–Co–N(2) | 82.24(14) | 84.51(17) | 86.31(13) | 83.2(2) | 85.26(13) |
| N(1)–Co–N(3) | 82.77(14) | 83.70(16) | 86.24(12) | 83.2(2) | 86.31(13) |
| N(1)–Co–O(1) | 89.90(13) | 88.70(15) | 90.75(11) | 91.7(2) | 90.30(12) |
| N(1)–Co–O(3) | 95.19(13) | 93.24(15) | 88.85(11) | 91.7(2) | 87.35(12) |
| N(1)–Co–O(W) | 176.54(14) | 176.42(17) | 178.20(12) | 180.0(2) | 177.53(13) |
| N(2)–Co–N(3) | 165.01(13) | 168.16(16) | 172.56(12) | 166.4(2) | 171.43(12) |
| N(2)–Co–O(1) | 87.41(12) | 88.36(14) | 85.76(10) | 88.3(2) | 86.57(11) |
| N(3)–Co–O(3) | 87.78(13) | 87.99(14) | 85.80(11) | 88.3(2) | 94.93(11) |
| O(1)–Co–O(W) | 86.92(13) | 88.81(17) | 89.22(11) | 88.3(2) | 91.80(12) |
| O(3)–Co–O(W) | 87.98(13) | 89.23(17) | 91.17(11) | 88.3(2) | 90.57(12) |
| N(2)–Co–O(3) | 93.82(12) | 91.52(14) | 93.97(10) | 91.7(2) | 93.90(11) |
| N(3)–Co–O(1) | 92.32(13) | 92.53(14) | 94.42(10) | 91.7(2) | 91.92(11) |
| N(2)–Co–O(W) | 98.94(13) | 92.84(16) | 91.89(12) | 96.8(2) | 93.56(14) |
| N(3)–Co–O(W) | 96.01(13) | 98.98(16) | 95.55(12) | 96.8(2) | 94.93(14) |
| O(1)–Co–O(3) | 174.88(12) | 178.03(14) | 179.54(10) | 176.6(2) | 177.55(12) |

[a]) The uncertainty on the last digit is given within parentheses.

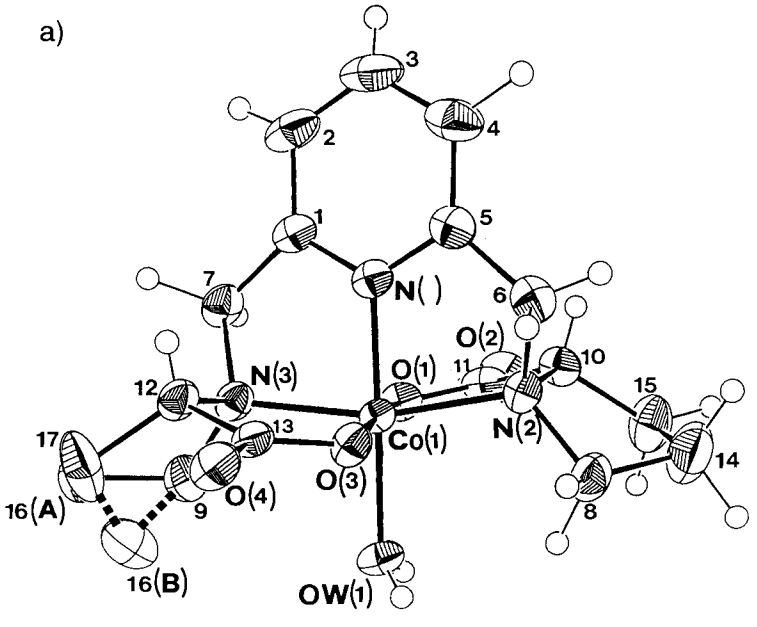

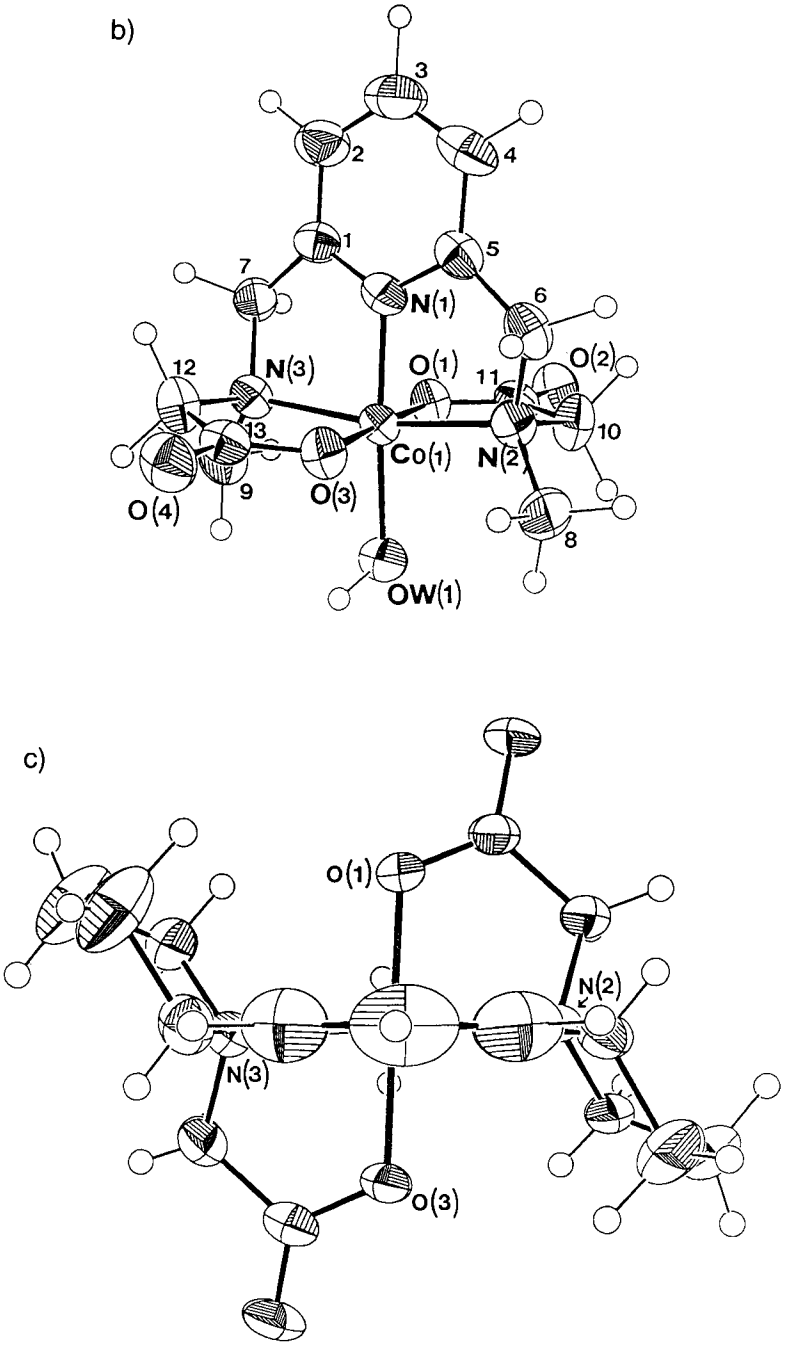


Fig. 2. *X-Ray crystal structure of the complexes* a) *[Co((S,S)-promp)$H_2O$]$ClO_4$*, b) *[Co(sarmp)$H_2O$]$ClO_4$, and* c) *[Co(*rac-*bapap)$H_2O$]$ClO_4$* (*Λ*-(*R*,*R*)-configuration represented)

with an occupancy of 0.5. Due to this fluxionality of only one five-membered ring, the $C_2$ symmetry is lost in the solid state. The bond lengths and angles of the two 'halves' of the molecule are not identical (see *Table 1*), whereas in the case of the *rac*-bamap complex they are. This asymmetry resembles that observed for the *meso*-Co(bamap) complex [6], where the loss of $C_2$ symmetry is due to the diastereoisomeric relationship of the two asymmetric C-atoms, relative to the absolute configuration of the complex. In the $^1$H-NMR spectrum of the latter complex, all the relevant signals are doubled. Such splitting is not observed in the $^1$H-NMR spectrum of [Co((*S*,*S*)-promp)$H_2O$]$^+$ (see *Experimental*), but the fluxional rate may be too high for more than an average signal to be seen.

The Co–N(1) bond length for the promp complex (1.843 Å) is similar to that found for (2,2′,6′,2′-terpyridyl)(carbonatohydroxo)cobalt(III) tetrahydrate [7] (1.846 Å) and [Co(*rac*-bamap)$H_2O$]$^+$ (1.838 Å). The Co–O(1) and Co–O(3) distances are similar to those determined for [Co(Hedta)$H_2O$] · 3 $H_2O$ [8]. The Co–O(W) bond (1.969 Å) is longer than those reported [8] [9] for [Co(Hedta)$H_2O$] · 3 $H_2O$ (1.917 Å) or Cs[Co($H_2O$)$_6$]($SO_4$)$_2$ · 6 $H_2O$ (1.873 Å). This bond stretching may be due to steric interactions between the protons of the pyrrolidine rings and the $H_2O$ molecule.

The ligand sarmp has no asymmetric C-atom and [Co(sarmp)$H_2O$]$ClO_4$, is a racemic mixture of the two enantiomers. The coordination sphere of Co in [Co(sarmp)$H_2O$]$^+$ (*Fig. 1, b*) is a distorted octahedral with a N(1)–Co–N(2) angle of 84.51°, and the pyridine ring twisted around the N(1)–N(2)–N(3) plane by 13.2°. The dihedral angle between the planes formed by N(2)–Co–O(1) and N(3)–Co–O(3) is 12.1° which indicates less distortion than for the promp complex where the dihedral angle is 16.0°. Unlike [Co(*rac*-bamap)$H_2O$]$^+$, the $C_2$ symmetry is lost in the solid state, as was observed for the promp complex. However, the $^1$H-NMR spectrum of [Co(sarmp)$H_2O$]$^+$ (see *Experimental*) indicates apparent $C_2$ symmetry in solution. The bond lengths and angles in [Co(sarmp)$H_2O$]$^+$ are quite similar to those determined for the promp and *rac*-bamap complexes. As there are no steric constraints, the Co–O(W) bond (1.919 Å) is very close to that for the *rac*-bamap complex (1.909 Å) and less than in the promp complex (1.969 Å).

An important feature of the structure of [Co(*rac*-bapap)]$ClO_4$ (*Fig. 2, c*) is the angle around the sixth coordination position. For example, the N(2)–Co–N(3) angle is 172.56°, and the O(1)–Co–O(3) angle is 179.54°, which are greater than for any of the other structures presented. This means less facile access to the sixth coordination site, with possible implications for inner sphere electron-transfer reactions between complexes of this type. The $CH_2$ groups are in a 'envelope' conformation, as for the promp complex, but no fluxionality was observed.

As only one of the two theoretically possible geometric isomers is isolated for the promp, sarmp, and bapap complexes, it can be concluded that coordination of these ligands to the Co centre is stereospecific. From the structure illustrated in *Fig. 2, a*, an absolute configuration of *Λ-exo* can be assigned to [Co((*S*,*S*)-promp)$H_2O$]$^+$ (and thus *Δ-exo* for its enantiomer [Co((*R*,*R*)-promp)$H_2O$]$^+$). An absolute configuration of *Δ*-(*S*,*S*) is assigned to the (–)-$_{436}$-enantiomer of the bapap complex, synthesized from (–)-2,6-bis(pyrrolidin-2-yl)pyridine, to which the absolute configuration of (*S*,*S*) was attributed [10]. The CD spectra of the fully characterized complexes can be compared with those synthesized with other stereospecific ligands. The CD spectra of [Co((*S*,*S*)-L)$H_2O$]$^+$

(L = alamp, bamap, bapap, and promp) are shown in *Fig. 3*. These spectra are in agreement with the assignment of *Λ* absolute configurations to the complexes of (*S*,*S*)-alamp, (*S*,*S*)-promp, (*S*,*S*)-bamap, and (*R*,*R*)-bapap.

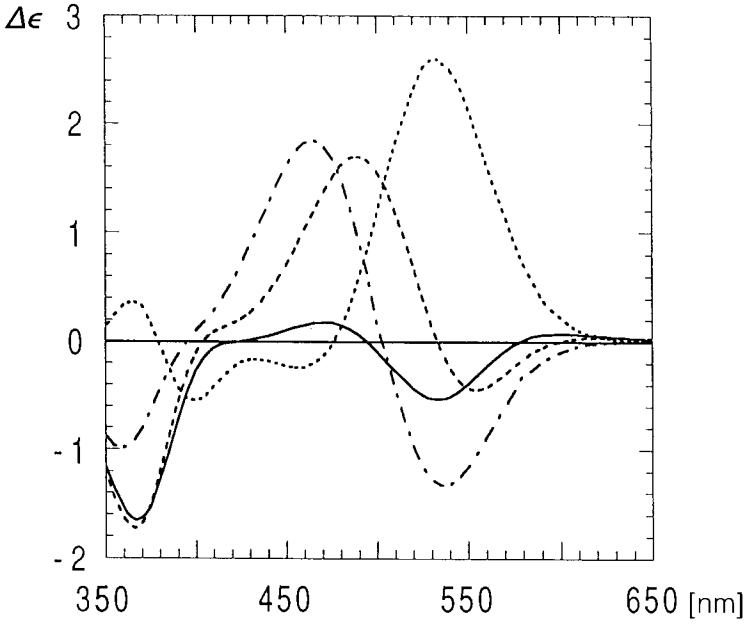


Fig. 3. *CD Spectra at 25°* of (——) *Λ-[Co((S,S)-bamap)H₂O]*$^{+}$; (–·–·–) *Λ*-exo*[Co((S,S)-alamp)H₂O]*$^{+}$; (– – –) *Λ*-exo-*[Co((S,S)-promp)H₂O]*$^{+}$; (---) *Λ-[Co((S,S)-bapap)H₂O]*$^{+}$

The ligand malmp proved to be a special case. The $^{1}$H-NMR and CD spectra of the $Co^{III}$ complex obtained by the usual procedure (see *Experimental*) indicated the presence of more than one compound. These could not be separated by ion-exchange chromatography with $NaClO_4$ as eluant or by fractional crystallization. Acidimetric titration of the mixture gave a molecular weight corresponding to the presence of one $H_2O$ molecule in the complex and a mean p*K* value of 8.1. Representation of $pH = f\{\log(a(1-a))\}$ gave a slope of 0.89, which showed that the p*K* values of the compounds were different. Complete separation of the mixture into two fractions (see *Experimental*) was achieved by ion-exchange chromatography at pH 8.1. Separate titrations of the two compounds (F-1 and F-2) gave p*K* values of 7.6 and 8.6, respectively. The CD spectra of both compounds and the X-ray crystal structure of *rac*-F-1 are shown in *Fig. 4*. Comparison of the structure and CD spectra with those illustrated in *Fig. 3* show that the absolute configuration of the F-1 fraction with (*R*,*R*)-malmp is *Λ-endo*. This difference can be explained by the fact that malmp has two pairs of neighbouring Me groups, on the N- and C(α)-atom of the aminocarboxylate moiety. To allow a staggered conformation of these vicinal Me groups, the substituents on the C(α)-atom, thus, occupy the less favourable *endo*-position. Unfortunately, the crystals of F-2 obtained were unsuitable for X-ray analysis. On the basis of the CD and NMR spectra, an *unsymmetric* configuration, with a peripheral arrangement of one of the aminocarboxylate rings is tentatively proposed for the F-2 compound.

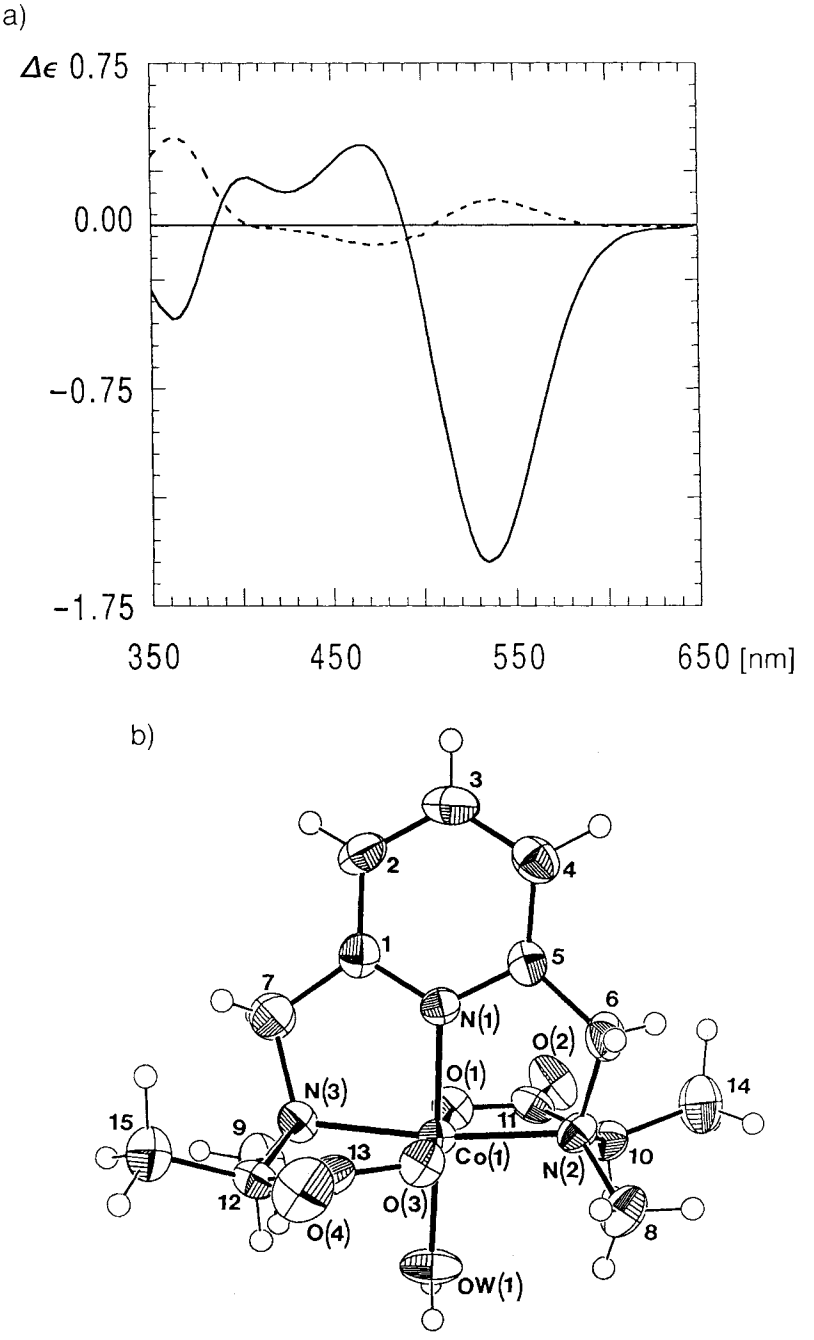


Fig. 4. a) *CD Spectra at 25° of the two fractions of [Co((*R,R*)-malmp)$H_2O$]$^+$.* (——): *Λ-endo*-[Co((*R,R*)-malmp)$H_2O$]$^+$, F-1; (---): *unsym-Λ-exo*-[Co((*R,R*)-malmp)$H_2O$]$^+$, F-2. b) *X-Ray crystal structure of F-1: [Co(*rac-*malmp)$H_2O$]$^+$.* (*Λ*-(*R,R*)-configuration represented).

In conclusion, it was found that for all ligands, except malmp, complex formation is stereospecific. For ligands with (*S*)-chirality, the absolute configuration is *Λ* for bamap, *Λ-exo* for alamp and promp, but *Δ* for bapap. The only exception is malmp, for which two compounds are formed: one with absolute configuration *Δ-endo-*(*S,S*) (or *Λ-endo-*(*R,R*)), and a second compound to which an *unsymmetric-Δ-exo-*(*R,R*)-structure has been attributed. The resolved X-ray structures, CD and NMR spectra support these assignments of the absolute configurations, which are represented in *Fig. 5*.

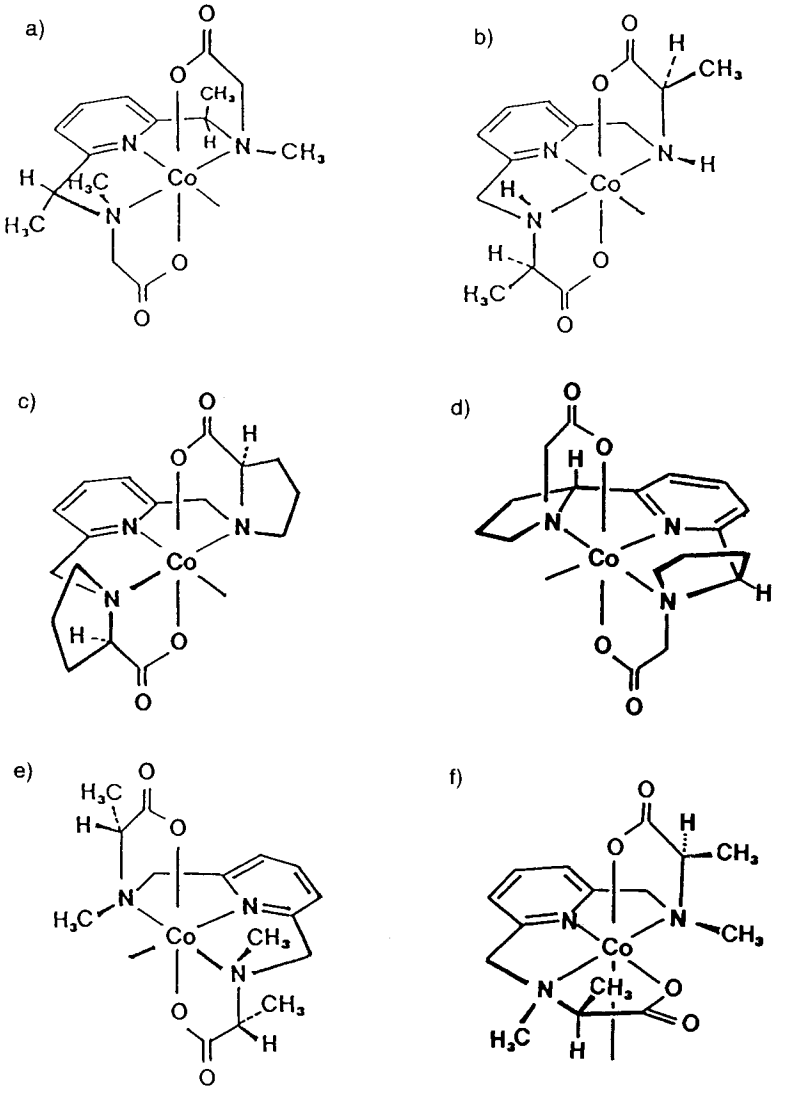


Fig. 5. *Absolute configurations of* a) *Δ-[Co((*R,R*)-bamap)$H_2O$]*$^+$; b) *Δ*-exo-*[Co((*R,R*)alamp)$H_2O$]*$^+$; c) *Δ*-exo-*[Co((*R,R*)-promp)$H_2O$]*$^+$; d) *Λ-[Co((*R,R*)-bapap)$H_2O$]*$^+$; e) *Λ*-endo-*[Co((*R,R*)-malmp)$H_2O$]*$^+$, *F-1*; f) unsym-*Δ*-exo-*[Co((*R,R*)-malmp)$H_2O$]*$^+$, *F-2*

2. *Equilibrium Measurements.* To understand and interpret the kinetics of electron transfer between complexes of $Co^{III}$ and $Fe^{II}$ as described in [11], it is important to determine their protonation and complex-formation constants with $Co^{II}$ and $Fe^{II}$. These constants were determined from potentiometric titration data, using the program SCOGS [12], and are reported in *Table 2*. A typical series of titration curves are illustrated in *Fig. 6* for the ligand sarmp. For $Fe^{II}$, the titration curve deviates at high pH due to formation of hydroxy species and dechelation of the complex. In all cases, the formation constant of the $Co^{II}$ complex is *ca.* 100 times greater than that of the corresponding $Fe^{II}$ complex, as would be expected from the *Irving-Williams* stability series [13]. In *Fig. 7*, the log of the stability constants for the $Co^{II}$ and $Fe^{II}$ complexes are plotted *vs.* the sum of the $pK_a$'s. The relationship is approximately linear, which indicates that complex formation is not unduly influenced by steric crowding at the ligand chelating sites.

Table 2. *Acid-Dissociation Constants for Various Pentadentate Ligands and Their $Fe^{2+}$ and $Co^{2+}$ Complex-Formation Constants at 25°. $\mu = 0.1$.*

| L | $pK_{a1}$ | $pK_{a2}$ | $\log K_{FeL}$ | $\log K_{CoL}$ | Ref. |
|---|---|---|---|---|---|
| sarmp | 8.15(4)[a]) | 9.35(2) | 10.44(4) | 12.27(4) | This work |
| bamap | 8.91(5) | 9.61(3) | 11.93(5) | 13.72(5) | [11] |
| malmp | 8.60(2) | 9.28(2) | 10.84(3) | 12.34(3) | This work |
| alamp | 8.23(2) | 9.02(2) | 9.62(7) | 11.70(3) | [11] |
| promp | 9.33(3) | 10.02(4) | 12.68(3) | 15.01(7) | This work |
| valmp | 8.03(4) | 9.28(4) | 10.05(5) | 11.80(5) | This work |

[a]) The uncertainty on the last digit is given within parentheses.

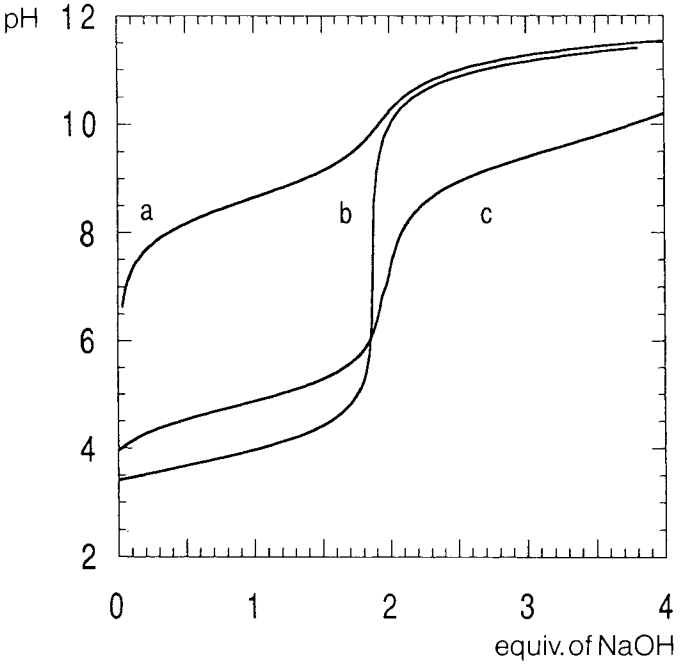


Fig. 6. *Titration curves at 25°.* $\mu = 0.1$ ($NaNO_3$) for sarmp. *a*) Free ligand; *b*) 1:1 ligand: $Co^{II}$ mixture; *c*) 1:1 ligand: $Fe^{II}$ mixture. [L] = $2 \cdot 10^{-3}$ M, [$Co^{II}$] = $2 \cdot 10^{-3}$ M, [$Fe^{II}$] = $2 \cdot 10^{-3}$ M.

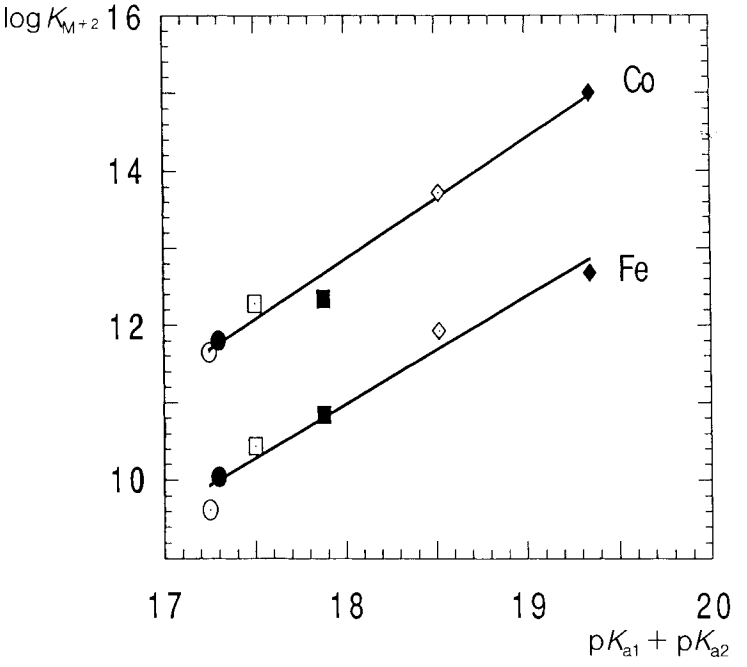


Fig. 7. *logs of the $Fe^{II}$ and $Co^{II}$ stability constants as a function of the sum of the acidity constants, $pK_{a1}$ and $pK_{a2}$*, for linear pentadentate ligands. o: alamp, ●: valmp, □: sarmp, ■: malmp, ◊: bamap, ♦: promp.

**Experimental.** – 1. *General.* Optical rotations: *Perkin-Elmer 241* polarimeter; CD measurements: *Jasco J-500* spectropolarimeter; UV/VIS spectra: *Uvikon 820* spectrophotometer; $^1$H-NMR spectra: *Bruker WP 200* ($^1$H: 200 MHz) and *AMX 400* ($^1$H: 400 MHz) spectrometers.

2. *Syntheses.* 2.1. *N,N′-[(Pyridine-2,6-diyl)bis(methylene)]bis[sarcosine] (sarmp).* Sodium sarcosinate was obtained by neutralization of an aq. soln. of 19.04 g (0.214 moles) of sarcosine by a stoichiometric amount of NaOH. 12.52 g (0.047 mol) 2,6-bis(dibromomethyl)pyridine (12.52 g, 0.047 mol) in 250 ml of distilled MeOH was added dropwise to 250 ml of a constantly stirred methanolic suspension of sodium sarcosinate at 50°. The mixture was then heated to 60°, the basicity maintained by addition of a methanolic soln. of 2M NaOH (phenolphthalein), and refluxed for 13 h. After evaporation to dryness, the yellowish residue was dissolved in $H_2O$, its pH adjusted to 6.5 with 2M HCl and adsorbed on a cation-exchange column (*Dowex 50X-8*, $H^+$). The column was washed with $H_2O$ until neutral, and the product eluted with 0.1M NaOH. All the fractions containing sarmp (TLC (silica gel, BuOH/AcOH/$H_2O$ 12:6:6), and UV spot) were collected and evaporated to dryness. The residue was recrystallized several times from an EtOH/acetone mixture. Sarmp is a white solid. Crude yield: 85%. Mol. wt. determined by spectrophotometric titration with $Cu^{II}$: found: 298.2 g; calc.: 281.3 g. $^1$H-NMR: (400 MHz, DMSO, reference TMS). 2.35 (*s*, 2 $CH_3N$); 3.28 (*s*, 2 $NCH_2COOH$); 3.83 (*s*, 2 $NCH_2$, py); 7.36 (*d*, 2 H, py); 7.78 (*t*, 1 H, py).

2.2. *N,N′-[(Pyridine-2,6-diyl)bis(methylene)]bis[(R)-proline] ((R,R)-promp).* Synthesis of the crude product using 0.22 mol of sodium (*R*)-prolinate and 0.073 mol of 2,6-bis(dibromomethyl)pyridine as described in [11]. After elution with NaOH from a column of *Dowex 50* ($H^+$), the soln. was acidified by addition of HCl and evaporated to dryness. promp · 2 HCl crystallized as fine needles in the refrigerator from a MeOH/acetone mixture. The compound was recystallized twice from MeOH/acetone. Yield: 56%. $[\alpha]^{r.t.}$ ($c$ = 0.35, $H_2O$) ($\lambda$): +60.8° (365), +23.7° (578). $^1$H-NMR: (200 MHz, $D_2O$, reference DSS): 2.25 (*m*, 3 $CH_2$, pyrollidine); 2.60 (*m*, $CH_2$, pyrollidine); 3.42 (*m*, 2 $H_{ax}$–C(1)); 3.87 (*m*, 2 $H_{eq}$–C(1)); 4.47 (*q*, 2 H); 4.69 (*d*, 2 $NCH_2$, py); 7.60 (*d*, 2 H, py); 8.00 (*t*, 1 H, py). Anal. calc. for $C_{17}H_{23}N_3O_4 \cdot 2$ HCl (406.3): C 50.24, H 6.20, N 10.34; found: C 50.06, H 6.16, N 10.26.

2.3. *N,N′-[(Pyridine-2,6-diyl)bis(methylene)]bis[(S)-proline] Dichlorohydrate ((S,S)-promp · 2 HCl).* Synthesized from 46.75 g (0.34 mol) of sodium (*S*)-prolinate and 22.6 g (0.085 mol) of 2,6-bis(dibromomethyl)-2,6-pyridine as described in *2.2.* $[\alpha]^{r.t.}$ ($c$ = 0.27, $H_2O$) ($\lambda$): −55.3° (365), −20.4° (578).

2.4. N,N′-*[(Pyridine-2,6-diyl)bis(methylene)]bis[*N-*methyl-(*S*)-alanine]* (*(*S,S*)-malmp*). Sodium *N*-methyl-L-alaninate was synthesized as described in [15]. Sodium *N*-methyl-L-alaninate (12.5 g, 0.1 mol) and 12.52 g (0.047 mol) of 2,6-bis(dibromomethyl)pyridine in 250 ml of MeOH were reacted as described in *2.1*. Crystallization of (*S,S*)-malmp from an EtOH/acetone mixture occurred on standing. M.p. 197°. Crude yield: 85%. $[\alpha]^{r.t.}$ ($c$ = 1.01, $H_2O$) ($\lambda$): −57.19° (365), −15.56° (578). $^1$H-NMR: (200 MHz, $D_2O$, reference DSS): 1.59 (*d*, 2 $CH_3CH_2$); 2.90 (*s*, 2 $CH_3N$); 3.95 (*m*, 2 $CH_3CH_2$); 4.59 (*m*, 2 $NCH_2$, py); 7.53 (*d*, 2 H, py); 7.98 (*t*, 1 H, py). Anal. calc. for $C_{15}H_{23}N_3O_4$ (309.4): C 58.24, H 7.49, N 13.58; found: C 58.14, H 7.74, N 13.50.

2.5. N,N′-*[(Pyridine-2,6-diyl)bis(methylene)]bis[*N-*methyl-(*R*)-alanine]* (*(*R,R*)-malmp*). Synthesized as described in *2.4* from 12.5 g (0.1 mol) of sodium *N*-methyl-D-alaninate and 12 g (0.045 mol) of 2,6-bis(dibromethyl)pyridine. M.p. 198°. $[\alpha]^{r.t.}$ ($c$ = 0.19, $H_2O$) ($\lambda$): +41.68° (365), +10.95° (578).

2.6. *2,2′-[Pyridine-2,6-diyl]bis[*rac-N-*(acetic acid)pyrrolidine]* (rac-*bapap*). Prepared as described in *2.1* from aq. solns. of 1.9 g (20 mmol) $ClCH_2COOH$ and 2.0 g (9 mmol) of *rac*-2,6-bis(pyrrolidinyl-2)pyridine (for preparation, *cf.* [14]): 2.5 g of a grey-white, hygroscopic product were obtained. It was used in its crude form for the synthesis of the $Co^{III}$ complex. Yield: 83%.

2.7. *2,2′-[Pyridine-2,6-diyl]bis[(*S*)-*N*-(acetic acid)pyrrolidine]* (*(*S,S*)-bapap*). Prepared as described in *2.6* from aq. solns. of 0.48 g (5.1 mmol) $ClCH_2COOH$ and 2.39 g (2.3 mmol) of (−)-2,6-bis(pyrrolidin-2-yl)pyridine [(+)-di-*O*-(*p*-toluyl)-D-tartrate], (for preparation, *cf.* [14]).

2.8. *Aqua{*N,N′-*[(pyridine-2,6-diyl)bis(methylene)]bis[sarcosine]}cobalt(III) Perchlorate (*[*Co(sarmp)* $H_2O$*]*$ClO_4$*)*. At 50°: 21.41 g (0.06 mol) of sarmp, in 300 ml of $H_2O$ were added to a vigourously stirred soln. of 28.4 g (0.1 mol) of $Na_3[Co(CO_3)_3 \cdot 3\ H_2O]$ and 2 g of activated charcoal (*Riedel-de-Haën*). The pH of the mixture was maintained at 6.5 for 24 h with glacial AcOH. The activated charcoal was eliminated and the mixture adsorbed on a *Sephadex* column (*SP C25*, $Na^+$). The neutral fraction was eluted with $H_2O$ and the cationic complex, eluted with 1% $NaClO_4$, was desalted on a column of *Sephadex SG10*. The quantity of $NaClO_4$ was checked by conductimetry. The desalted fraction was evaporated almost to dryness, heated until completely redissolved, and left to crystallize at r.t. Large, dark-red needles of $[Co^{III}(sarmp)H_2O]ClO_4$ were filtered and washed in distilled EtOH. Yield: 34.4%. $^1$H-NMR (400 MHz, DMSO, reference TMS) 2.89 (*s*, 2 $CH_3N$); 3.85 (*d*, 2 $NCH_2COO$); 4.74 (*d*, 2 $CH_2N$); 7.66 (*d*, 2 H, py); 8.19 (*t*, 1 H, py). Anal. calc. for $C_{13}H_{19}CoN_3O_5 \cdot ClO_4$ (455.4): C 34.25, H 4.17, N 9.22; found: C 34.06, H 4.35, N 9.06.

2.9. *Aqua{*N,N′-*[(pyridine-2,6-diyl)bis(methylene)]bis[(*R*)-proline]}cobalt(III) Perchlorate (*[*Co((*R,R*)-promp)* $H_2O$*]*$ClO_4$*)*. Synthesized as described in *2.8* from 4.48 g (1.1 mmol) of (*R,R*)-promp·2 HCl and 4.11 g (1.35 mmol) of $Na_3[Co(CO_3)_3 \cdot 3\ H_2O]$. Yield: 21%. $[\alpha]^{r.t.}$ ($\lambda$): +1480.5° (365), +144.7° (578). $^1$H-NMR: (200 MHz, $D_2O$, reference DSS). 2.07 (*m*, 4 H, pyrrolidine); 2.29 (*m*, 4 H, pyrrolidine); 2.62 (*m*, 2 H, pyrrolidine); 3.24 (*m*, 2 H, pyrrolidine); 4.01 (*d*, NC*H*$CH_2COOH$); 4.72 (*AB* system, 2 $NCH_2$–py); 5.10 (*AB* system, 2 $NCH_2$(b)–py); 7.77 (*d*, 2 H, py); 8.22 (*t*, 1 H, py).

2.10. *Aqua{*N,N′-*[(pyridine-2,6-diyl)bis(methylene)]bis[(*S*)-proline]cobalt(III) Perchlorate (*[*Co((*S,S*)-promp)* $H_2O$*]*$ClO_4$*)*. Synthesized as described in *2.9* from 4.60 g (1.12 mmol) of (*S,S*)-promp·2 HCl and 4.5 g (1.48 mmol) of $Na_3[Co(CO_3)_3 \cdot 3\ H_2O]$. $[\alpha]^{r.t.}$ ($\lambda$): −1595.5° (365), −194.2° (578). The *rac*-complex was obtained by mixing equimolar quantities of the (*R,R*)- and (*S,S*)-complexes, followed by recrystallization.

2.11. *Aqua{*N,N′-*[(pyridine-2,6-diyl)bis(methylene)]bis[(*R*)-*N*-methylalanine]}cobalt(III) Perchlorate (*[*Co((*R,R*)-malmp)* $H_2O$*]*$ClO_4$*)*. Synthesized as described in *2.8* from 1.85 g (6 mmol) of (*R,R*)-malmp and 2.34 g (6.5 mmol) $Na_3[Co(CO_3)_3 \cdot 3\ H_2O]$. NMR and CD spectra of the crystallized complex indicated the presence of more than one compound. An aq. soln. containing *ca.* 0.5 g of the mixture obtained from the synthesis was put on an ion-exchange column (*Sephadex SP-25*, $Na^+$) and washed with $H_2O$. On elution with a 0.05M $Na_2HPO_4$ buffer soln. at pH 8.1 (adjusted with HCl), two clearly distinct bands of comparable magnitude developed, and could be collected, and completely separated from the column. The two components, called F-1 and F-2, in their elution order, were treated separately to eliminate the buffer: the pH is fixed at 3–4 with HCl, the soln. put on a *Sephadex SP-25* ion-exchange column, and eluted with 1% $NaClO_4$. The fractions containing the complex were concentrated to *ca.* 50 ml, and the excess perchlorate was eliminated by elution with $H_2O$ on a column of *Sephadex G10* ($d$ = 4 cm, $I$ = 120 cm). Whereas F-2 crystallized as the perchlorate salt from a small volume of the aq. soln., the F-1 perchlorate crystallized only by complete evaporation over $H_2SO_4$ in a dessicator. The purity of the compounds was tested by acidimetric titraton: $[Co(C_{13}H_{19}N_3O_5)]ClO_4$, mol. wt. = 455.7 g. F-1 (447.5 g): F-2 (468.9 g). Separate chromatography of both compounds at pH 8.1 showed that no interconversion between the two isomers took place during the various separation operations.

2.12. *Aqua{*N,N′-*[(pyridine-2,6-diyl)bis(methylene)]bis[(*S*)-*N*-methylalanine]}cobalt(III) Perchlorate (*[*Co((*S,S*)-malmp)* $H_2O$*]*$ClO_4$*)*. Synthesized and separated as described in *2.11* from 2 g (6.47 mmol) of (*S,S*)-malmp and 2.34 g (6.47 mmol) $Na_3[Co(CO_3)_3 \cdot 3\ H_2O]$. Yield: 15%. $[\alpha]^{r.t.}$ ($c$ = 0.0136, $H_2O$) ($\lambda$): −30.15° (365),

Table 3. *Crystal Data and Experimental Details for $Co^{III}$ Complexes with Stereospecific Linear Pentadentate Ligands*

| Ligand | sarmp | promp | bapap | malmp |
|---|---|---|---|---|
| Empirical formula | $C_{13}H_{17}N_3O_4Co \cdot H_2O \cdot ClO_4$, 2.25 $H_2O$ | $C_{17}H_{21}N_3O_4Co \cdot H_2O \cdot ClO_4$ | $C_{17}H_{21}N_3O_4Co \cdot H_2O \cdot ClO_4$, $H_2O$, $C_2H_5OH$ | $C_{15}H_{21}N_3O_4Co \cdot H_2O \cdot ClO_4$, 1.5 $H_2O$ |
| $M_r$ | 533.8 | 553.8 | 571.9 | 510.8 |
| Crystal color/habit | red blocks | red rods | red plates | red square rods |
| Crystal system | monoclinic | monoclinic | triclinic | monoclinic |
| Space group | $P21/n$ | $P2_1$ | $P\bar{1}$ | $A2/n$ |
| $Z$ | 4 | 2 | 2 | 8 |
| $D_c$ [g/cm$^3$] | 1.614 | 1.686 | 1.555 | 1.647 |
| Linear absorption coefficient $\mu(MoK_\alpha)$ [cm$^{-1}$] | 10.2 | 10.4 | 8.7 | 20.2 |
| Crystal dimensions [mm] | 0.61 × 0.49 × 0.32 | 0.46 × 0.23 × 0.19 | 0.46 × 0.21 × 0.13 | 0.49 × 0.21 × 0.19 |
| Cell parameters: | | | | |
| No. reflections | 18 | 31 | 23 | 18 |
| 2$e$ range [°] | 28–35 | 18–28 | 28–35 | 28–34 |
| $a$ [Å] | 8.431(1) | 11.983(2) | 8.376(1) | 14.615(2) |
| $b$ [Å] | 23.402(2) | 7.237(1) | 10.449(2) | 19.816(2) |
| $c$ [Å] | 10.555(1) | 12.013(2) | 14.876(2) | 15.159(1) |
| $\alpha$ [°] | | | 107.05(1) | |
| $\beta$ [°] | 106.11(1) | 106.20(1) | 99.12(1) | 110.24(19) |
| $\gamma$ [°] | | | 93.25(1) | |
| $V$ [Å$^3$] | 2039.9(4) | 1000.4(3) | 1221.6(3) | 4119.1(8) |
| Scan mode | $\omega/\theta$ | $\omega/\theta$ | $\omega/\theta$ | $\omega/\theta$ |
| $\theta_{max}$ [°] | 25 | 27.5 | 25 | 25 |
| $h,k,l$ range | ±10, +27, +12 | ±15, +9, +15 | ±9, +12, ±17 | ±17, +23, +18 |
| No. of reference reflections | 3 | 4 | 2 | 3 |
| and variation [%] | 3.5 | 5.0 | 2.5 | 2.0 |
| No. reflections measured | 3587 | 2621 | 4314 | 3636 |
| No. unique reflections | 3587 | 2508 | 4304 | 3636 |
| No. of reflections used in refinement | 2699 | 2351 | 3098 | 2510 |
| $[I > x\sigma(I)]$, where $x$ = | 3.0 | 2.5 | 3.0 | 2.5 |
| No. parameters refined | 295 | 348 | 420 | 387 |
| $R$ | 0.054 | 0.035 | 0.038 | 0.038 |
| $wR$ | 0.089 | 0.050 | 0.056 | 0.057 |
| $w^{-1} = \sigma^2(F_0) + k(F_0^2)$, where $k$ = | 0.005 | 0.0015 | 0.001 | 0.003 |
| max shift/sigma ratio | 0.263 | 0.415 | 0.179 | 0.051 |
| Residual density: max [e/Å$^3$] | 1.36 | 0.87 | 0.51 | 0.31 |
| min [e/Å$^3$] | –0.70 | –0.38 | –0.36 | –0.47 |

+46.32° (578). $^1$H-NMR: (200 MHz, $D_2O$, reference DSS). 1.56 (*d*, 2 $CH_3CH$); 3.09 (*s*, 2 $CH_3N$); 4.28 (*dd*, 2 $NCHCH_3$); 4.87 (*dd*, *AB* system, 2 $CH_2$); 7.60 (*d*, 2 H, py); 8.12 (*t*, 1 H, py). The *rac*-complexes of F-1 and F-2 were obtained by mixing equimolar quantities of the corresponding (*R,R*)- and (*S,S*)-complexes, followed by recrystallization in $H_2O$.

2.13. *Aqua{2,2'-[pyridine-2,6-diyl]bis[* rac-*(acetic acid)pyrrolidine]}cobalt(III) Perchlorate ([Co(* rac-*bapap)$H_2O$]$ClO_4$)*. Synthesized as described in *2.8* from 2.0 g (6 mmol) of *rac*-bapap and 2.6 g (7 mmol) $Na_3[Co(CO_3)_3 \cdot 3\ H_2O]$. Crystallized from $H_2O$/EtOH. X-Ray analysis showed the presence of one molecule of EtOH per molecule of complex. Anal. calc. for $C_{17}H_{21}CoN_3O_4 \cdot ClO_4 \cdot H_2O \cdot EtOH$ (571.85): C 39.91, H 5.46, N 7.35; found: C 40.48, H 5.40, N 7.46.

2.14. *Aqua{2,2'-[pyridine-2,6-diyl]bis[(*S*)-(acetic acid)pyrrolidine]}cobalt(III) Perchlorate ([Co((*S,S*)-bapap)$H_2O$]$ClO_4$)*. Synthesized as described in *2.13* from 0.76 g (2.3 mmol) (*S*)-bpp (for preparation, *cf.* [14]) and 0.85 g (2.3 mmol) $Na_3[Co(CO_3)_3 \cdot 3\ H_2O]$. Efforts to crystallize the compound were unsuccessful. The concentration of a known soln. was determined by UV/VIS spectroscopy.

3. *Potentiometric Measurements.* All solns. were prepared with bidistilled $H_2O$. Titration curves were measured at 25.0 ± 0.1°, under $N_2$ using 0.01M NaOH as titrant. $[M^{2+}]$ and $[L^{2-}] \approx 2.5 \cdot 10^{-3}$ M, $\mu = 0.1$ ($NaNO_3$). The dissociation and equilibrium constants were determined using the program SCOGS [12].

4. *X-Ray measurements* were accomplished using a *Stoe AED2* four-circle diffractometer with graphite monochromated Mo$K_\alpha$ radiation. The crystal data and experimental details are given in *Table 3*. The structures were solved by *Patterson* and *Fourier* methods, using the NRCVAX system [16] which was also used for all further calculations. In all four complexes, the majority of the H-atoms were located from difference maps and refined isotropically. In the sarmp complex, the perchlorate O-atoms undergo considerable thermal motion. In the promp complex, two alternative positions were found for atom C(16). Both positions were included with occupancies of 0.5. The H-atoms at C(7) were included in calculated positions and held fixed, $U_{iso} = 0.0431$ Å$^2$. H-Atoms at C(9), C(16a), C(16b), and C(17) were included for both conformations of the five-membered ring with occupancies of 0.5, $U_{iso}$0.04 Å$^2$ and held fixed. In the malmp complex, the second perchlorate anion was disordered with atom O(21) sitting on a two-fold axis. Atom Cl(2) was moved off the two-fold axis and given an occupancy of 0.5 and allowed to refine. Atoms O(22) and O(23) have occupancies of 1.0 and 0.5, respectively.

Neutral complex-atom scattering factors in NRCVAX are from [17]. Selected distances and angles are given in *Table 1*, and the numbering schemes used are illustrated in the ORTEP [18] plots of the cations (*Figs. 2* and *4, b*). Final positional and equivalent isotropic thermal parameters, together with full distances and angles, have been deposited with the *Cambridge Crystallographic Data Centre*, Cambridge, England.

We are very grateful to the *Swiss National Science Foundation* for financial support, grants No. 26-464.89 and 20-231164.91.

## REFERENCES

[1] K. Bernauer, S. Bourqui, D. Hugi-Cleary, R. Warmuth, *Helv. Chim. Acta* **1992,** *75,* 1288.
[2] K. Bernauer, *Metal Ions Biolog. Syst.* **1991,** *27,* 265.
[3] A. G. Lappin, R. A. Marusak, *Coord. Chem. Rev.* **1991,** *109,* 125.
[4] D. A. Geselowitz, H. Taube, *J. Am. Chem. Soc.* **1980,** *102,* 4525.
[5] K. Bernauer, P. Pousaz, *Helv. Chim. Acta* **1984,** *67,* 796.
[6] H. Stoeckli-Evans, L. Brehm, P. Pousaz, K. Bernauer, H. Bürgi, *Helv. Chim. Acta* **1985,** *68,* 185.
[7] E. S. Kucharski, B. W. Shelton, A. H. White, *Aust. J. Chem.* **1978,** *31,* 47.
[8] H. Okazaki, K. Tokoimaka, H. Yoneda, *Inorg. Chem. Acta* **1983,** *74,* 169.
[9] J. K. Beatties, *J. Chem. Soc., Dalton Trans.* **1981,** 2105.
[10] K. Bernauer, F. Gretillat, H. Stoeckli-Evans, R. Warmuth, submitted.
[11] K. Bernauer, P. Pousaz, J. Porret, A. Jeanguenat, *Helv. Chim. Acta* **1988,** *71,* 1339.
[12] H. S. Stünzi, SCOGS, in 'Computational Methods for the Determination of Formation Constants', Ed. D. L. Leggett, Plenum Press, 1985.
[13] J. E. Huheey, 'Inorganic Chemistry', Harper and Row, 1975, p. 225.
[14] K. Bernauer, F. Gretillat, *Helv. Chim. Acta* **1989,** *72,* 477.
[15] P. Quitt, J. Hellerbach, K. Vogel, *Helv. Chim. Acta* **1963,** *46,* 327.
[16] E. J. Gabe, Y. le Page, J.-P. Charland, F. L. Lee, NRCVAX, *J. Appl. Crystallogr.* **1989,** *22,* 384.
[17] International Tables for X-Ray Cystallography, Kynoch Press, Birmingham, England, 1974, Vol. IV.
[18] C. K. Johnson, ORTEP-II, Report 5138, Oak Ridge National Laboratory, Oak Ridge, Tennessee, USA.